Biomaterials 51 (2015) 108–118

Contents lists available at ScienceDirect

Biomaterials

journal homepage: www.elsevier.com/locate/biomaterials

Histopathological and biomechanical evaluation of tenocyte seeded allografts on rat Achilles tendon regeneration

Cansın Güngörmüş [a, *], Dürdane Kolankaya [a], Erkin Aydin [b]

[a] Hacettepe University, Faculty of Science, Biology Department, Zoology Section, Beytepe, Ankara, 06120, Turkey
[b] Abdullah Gul University, Department of Materials Science and Nanotechnology Engineering, Asik Veysel Bulvari, Erciyes Teknopark 4/67A, Melikgazi, Kayseri, 38039, Turkey

ARTICLE INFO

Article history:
Received 4 November 2014
Accepted 25 January 2015
Available online 17 February 2015

Keywords:
Tendon
ECM (extracellular matrix)
Gene expression
Immunochemistry
Mechanical properties

ABSTRACT

Tendon injuries in humans as well as in animals' veterinary medicine are problematic because tendon has poor regenerative capacity and complete regeneration of the ruptured tendon is never achieved. In the last decade there has been an increasing need of treatment methods with different approaches. The aim of the current study was to improve the regeneration process of rat Achilles tendon with tenocyte seeded decellularized tendon matrices. For this purpose, Achilles tendons were harvested, decellularized and seeded as a mixture of three consecutive passages of tenocytes at a density of 1×10^6 cells/ml. Specifically, cells with different passage numbers were compared with respect to growth characteristics, cellular senescence and collagen/tenocyte marker production before seeding process. The viability of reseeded tendon constructs was followed postoperatively up to 6 months in rat Achilles tendon by histopathological and biomechanical analysis. Our results suggests that tenocyte seeded decellularized tendon matrix can significantly improve the histological and biomechanical properties of tendon repair tissue without causing adverse immune reactions. To the best of our knowledge, this is the first long-term study in the literature which was accomplished to prove the use of decellularized matrix in a clinically relevant model of rat Achilles tendon and the method suggested herein might have important implications for translation into the clinic.

1. Introduction

Tendon is a highly specialized fibrous tissue whose function is to transfer mechanical forces between muscle and bone. Therefore, it has evolved to have toughness to resist tensile loads and elasticity to withstand both repetitive as well as constant loading. These extraordinary biomechanical properties of tendon are attributable to the highly organized extracellular matrix (ECM) components consisting dominantly type I collagen fibrils, type III and type V collagens, proteoglycans, elastin and fibronectin; and tenocytes embedded within this network of matrix [1–3].

The incidence of human Achilles tendon rupture was reported as 12–18/100,000/year in recent studies [4–6]. However, tendon injuries in humans as well as in veterinary medicine are problematic because tendon has a poor regenerative capacity and complete regeneration of the ruptured tendon is never achieved [7]. Despite remodeling, the histological and mechanical properties of naturally healed tendon tissue never match those of intact tendon because the remodeling of naturally healed tissue is not extensive but it is basically deposition of scar tissue at the site of injury. Current standard of care for tendon injury is either surgical or conservative route. Surgical treatment involves the removal of inflamed, devitalized or contaminated tissue from the lesion site by a number of incisions while conservative treatment only involves medical support accompanying exercise without any surgical protocol. In the literature, several synthetic and natural origin biomaterials including poly-glycolic acid (PGA), poly-lactic glycolic acid (PLGA), nylon, silicone, carbon fibers, Dacron grafts chitosan and collagen derivatives were evaluated as an augment for tendon regeneration [8–18]. However, most of these applications were reported to cause notable inflammatory responses and frequent complications leading to postoperative scar formation and adhesions between tendon and the surrounding tissues due to limited biocompatibility and/or functional compatibility [10,13].

Recently, regenerative medicine has been emerging as an alternative in tendon repair. Several approaches have been developed to improve tendon healing such as stem cell injection, gene

* Corresponding author. Tel.: +90 312 327 41 81; fax: +90 312 327 41 56.
E-mail addresses: cansingungormus@gmail.com (C. Güngörmüş), durdane@hacettepe.edu.tr (D. Kolankaya), erkin.aydin.1@gmail.com (E. Aydin).

http://dx.doi.org/10.1016/j.biomaterials.2015.01.077
0142-9612/

transfer and growth factor injection into the site of injury [19–23]. Awad [22] reported that mesenchymal stem cells (MSCs) suspended in type I collagen gel may not be adequate for patellar tendon regeneration in rabbits because of the "non-aligned" structure of collagen matrix, which probably effected the histological disorganization of the recovering tendon. Furthermore, Doroski [21] reported that use of MSCs for their potential to differentiate into tenocytes may be hampered by the fact that they have the ability differentiate into other related cell types as well. Several growth factors including BMP, TGF-β, bFGF and PDGF have been shown to enhance wound healing process, increase cell proliferation and collagen production in rat tendon [23–25]. However, during the wound healing process, available growth factor concentration has to be precisely balanced so that it is neither insufficient to cause failure to induce repair nor excess to cause adhesion of the skin on tendon scar surface and the loss of normal tendon function [26]. *In vivo* gene transfer approach is also known to have major disadvantages such as the adversity of finding vectors with high transgenic activity, immune response development against vectors, and general safety concerns as in all gene therapy applications [27–29].

Tissue engineering is a promising alternative in tendon repair when applied in conjunction with decellularized extracellular matrices (DCM). However, donor site scarcity and morbidity limit the extensive use of autografts as DCM in tendon repair [30]. Alternatively, xenogenic DCM has been reported to improve tendon regeneration [31–33]. Nevertheless, current experience in the preparation of xenogenic grafts has shown that these grafts may instigate inflammatory responses and require a longer recovery period to integrate into native tissue [34]. In clinical practice, use of cadaveric DCM may therefore be a more viable alternative than auto − or xenografts.

Use of allograft DCM started attracting attention in several tissue engineering applications, including kidney, liver and lung reconstruction [35–38]. In allogenic tendon tissue engineering, current approaches involve seeding dermal fibroblasts, tenocytes, mesenchymal and bone marrow (BMSC) stem cells onto DCM as allogeneic tendon grafts, which has shown an improved healing [22,34,39]. In these cases, it is reported that the functional recovery of ruptured tendon is established earlier and the healing is accelerated with rapid remodeling.

In this study, it was hypothesized that DCM with seeded tenocytes improve regeneration process during Achilles tendon healing in rats. For this purpose, Achilles tendons were harvested, decellularized and seeded with tenocytes. Specifically, tenocytes were passaged 3 times to gain sufficient amount of cells to construct DCM + Tenocyte composites that were further transplanted to DCM + Tenocyte group. The viability of reseeded tendon constructs was followed postoperatively up to 6 months using histopathological and biomechanical analysis. To the best of our knowledge, this is the first long term study in the literature which investigated the effects of DCM seeded with previously characterized tenocytes both phenotypically and genotypically on tendon regeneration in rats.

2. Materials and methods

Adult male *Rattus norvegicus (Wistar albino)* rats (250 ± 50 g) (n = 50 as tenocyte and decellularized tendon source and n = 30 for *in vivo* experiments) were used. All experimental procedures and the use of animals were approved by Hacettepe University Animal Ethical Committee (Approval Number: 2009/8). Animals were reared on a basal diet with water *ad libitum* and maintained in an air-conditioned room at 22.4 ± 1.6 °C, in a relative humidity of 47.2 ± 1 and 12 h light/dark cycle.

2.1. Tenocyte isolation and culture

The rats were sacrificed by CO_2 asphyxiation. The tendon tissue was removed and rinsed in sterile phosphate-buffered saline (PBS) containing penicillin. Tendon segments were placed in six-well culture plates for explant culture in DMEM/F12 growth medium (SID8437) supplemented 10% fetal bovine serum (FBS) (SIF6178), 1% glutamine-penicillin-streptomycin (SIG6784).

Tenocytes were obtained and cultured in accordance with the literature [39,40]. Tenocytes from three consecutive passages were mixed together to obtain sufficient number of cells for immunofluorescence staining and qPCR studies and to construct DCM + Tenocyte composites to be transplanted to DCM + Tenocyte group (n = 30 and 1 × 10^6 cells/animal).

2.2. Cell proliferation and senescence

Viable cells from the first, second, and third passage (P1, P2, P3, respectively) were counted using digital cell counter (Beckmann, Vicell, USA). The number of viable cells was plotted against culture day to generate a growth curve for each passage.

Before seeding tenocytes on DCM surface, cell senescence of P1, P2 and P3 tenocytes was determined using the β-galactosidase activity staining assay with Senescence Cell Histochemical Kit (Sigma) according to the manufacturer's guidelines to obtain if passaging caused any senescence. Digital images were captured with AXIO Vision.4B Software Olympus IX70 (Olympus Corporation, USA).

2.3. Immunofluorescence staining

Before seeding, cells from consecutive passages were compared for their collagen/tenocyte marker production by immunofluorescence staining and qPCR. P1, P2, and P3 tenocytes were fixed with 2.5% glutaraldehyde. For antigen retrieval, tenocytes were incubated with Triton X − 100 (Merck, New Jersey, USA). Cells were incubated with primary antibodies (Santa Cruz Biotechnology, Inc., Heidelberg, Germany) against collagen type I/type II (sc25974 − sc7764), collagen type III/type V (sc8781 − sc9856), tenomodulin/tenascin − C (sc49325 − sc9871) and biotin-labeled secondary antibodies (Vectorlabs, California, USA) for double staining. Detection was performed using the Vectastain ABC Kit, FITC (A2001) and Texas Red (A2002) fluorochromes (Vectorlabs, California, USA). Digital images were acquired with AXIO Vision.4B Software and Olympus IX70 (Olympus Corporation, USA).

2.4. Gene expression analysis with quantitative, real-time PCR (qPCR)

Total RNA from 1.5 × 10^6 tenocytes was extracted with Tri Reagent according to the manufacturer's directions (Sigma, UK). First-strand complementary DNA (cDNA) was synthesized with cDNA kit (Roche, Applied Science, Germany) according to the manufacturer's protocol.

Primers were designed with Perl-Primer software (Sourceforge.Net) and obtained from Metabion International, Martinsried, Germany. Primer sequences are given in Table 1. Specificity of all primers was confirmed by a single product amplification using melting curve analysis.

qPCR assays were performed in triplicate to obtain relative expression levels for each gene. Expressions of target genes in cell samples belonging to each passage (P1, P2 and P3) were compared to *Gapdh* expression -as internal control- and data analysis was performed according to a previously reported formulation [41].

Gene expression patterns were obtained by using Roche 480 Sybr Green I Master Kit with Light Cycler 480 (Roche, Applied Science, Germany). The reaction mixture consisted of 2 μL cDNA, 0.5 μmol/l of each primer, 200 μmol/l each dNTP, 1.5–2 mmol/l MgCl2, 2.5 μL 10× reaction buffer, 0.05 IU/μL *Taq* DNA polymerase and 17.3 μL distilled water. In addition, SYBR Green, a double-stranded DNA dye, was used. The cDNA was denatured by heating to 95 °C for 1 min. The template was amplified for 40 cycles of denaturation for 30 s at 95 °C, annealing of primers at 60–65 °C for 1 min and extension at 72 °C for 30 s. PCR products were identified by generating a melting curve. The melting protocol consisted of heating the samples to 95 °C for 10 min, followed by cooling to 65 °C for 1 min and slowly heating to 95 °C while monitoring SYBR Green fluorescence.

Table 1
Sequence of primers used in qPCR.

Target gene	Primer	Sequence	GC%	Tm °C
Col1	Forward	5′-AGT CGA TTC ACC TAC AGC AC-3′	50	58
	Reverse	5′-GCC AAT GTC CAT TCC GAA-3′	50	54
Col2	Forward	5′-CAG CAG GTT CAC GTA CAC T-3′	52	64
	Reverse	5′-GAG GTC TTC TGT GAT CGG T-3′	52	64
Col3	Forward	5′-CAA ATT CAC TTA CAC AGT TCT A-3′	31.80	55
	Reverse	5′-ATG TCA TAG GGT GCG ATA-3′	44.4	52
Col5	Forward	5′-AGT ATC CAC TCT TCC CTG-3′	50	54
	Reverse	5′-GAG GAT CAA GGT GAC ATT-3′	44.4	50
Tnsc	Forward	5′-GTG GCT GCA TTG ATG GTT G-3′	60	63
	Reverse	5′-TCT CAG CAT GGT CAC CTC C-3′	50	58
Tnmd	Forward	5′-CAA AGA ATC CTC CAG AGA A-3′	42.1	53
	Reverse	5′-CAG GAC AAT TAG AGT TAA GG-3′	40	54
Gapdh	Forward	5′-TAT GAC TCT ACC CAC GGC AA-3′	50	58
	Reverse	5′-GAC TCC ACG ACA TAC TCA GCA-3′	52.4	61

2.5. Decellularization of Achilles tendons

Harvested Achilles tendons were washed with PBS and frozen at −80 °C until use. Before use, tendons were thawed and placed in six-well culture plates containing 0.05% Trypsin − EDTA for 24 h at 37 °C. The Trypsin − EDTA was then discarded and tendons were placed in 0.5% Triton X − 100 for 24 h at room temperature. All tendons were stained with DAPI and examined under fluorescent microscope (Olympus IX70, USA) to confirm decellularization.

2.6. Reseeding of decellularized tendons in vitro

Decellularized tendons were washed in PBS containing penicillin − streptomycin and DMEM/F12. Each decellularized tendon was reseeded with tenocytes at a density of 1×10^6 cells/ml in a 96 well plate by immersion of the tendons in DMEM/F12 containing media. Cell suspensions were prepared with serum-free DMEM/F12. The cell–scaffold constructs were then incubated at 37 °C in a humidified incubator with 5% CO_2 for 48 h. After making sure that cells from consecutive passages had practically the same properties in terms of cellular senescence, cells were further analyzed with immunofluorescence staining and qPCR. According to the results which shows that different passages have similar collagen/tenocyte marker production; cells from P1, P2 and P3 were mixed together to have sufficient number of cells for reseeding on DCMs.

2.7. In vivo implantation of reseeded tendon constructs

The summary of all experimental groups is given in Table 2. The rats were anesthetized with intraperitonal injection of 2 mg/kg xylazine HCl and 15 mg/kg ketamine HCl. The skin was sterilized with 10% poviodine solution.

A longitudinal incision was made on the skin above gastrocnemius muscle to calcaneus (heel) bone. The surgical protocol was modified for control and experimental groups. In Control Group, mid 1/3 portion of the Achilles tendon was cut from both ends and immediately sutured back with 8-0 absorbable polydioxanone at both proximal and distal ends. In Decellularized Matrix Control Group (DCM − Control), mid 1/3 portion of the Achilles tendon was cut from both ends and removed. An immediate interpositioning DCM of the same length was sutured proximally and distally with 8-0 absorbable polydioxanone (Ethicon, Woluwe, Belgium). In DCM + Tenocyte Group, mid 1/3 portion of the Achilles tendon was cut from both ends and removed. An immediate interpositioning DCM of the same length consisting of reseeded tenocytes was sutured proximally and distally with 8-0 absorbable polydioxanone. All surgery areas were partially immobilized to prevent the loading of the repaired tendon according to the previously reported protocol [42].

Grafted tendons were harvested from each experimental group at 2, 4, 6, 8, 12 and 24 weeks after surgery. From each rat, two samples − one from each leg − were obtained. In each rat the right Achilles tendon served as sample for histopathological analysis sample, while the contralateral served as sample for biomechanical analysis.

2.8. Histopathological analysis

Each harvested tissue was fixed in 10% formaldehyde for 24 h. Specimens were embedded in paraffin wax and 5 μm-thick longitudinal sections were taken using Leica RM 2125 microtome. The sections were stained with hematoxyline eosin (H & E) and examined independently by two blinded observers through light microscopy (Leica DM3000). A histological scoring system previously designed by Stoll [12] was applied to each sample to evaluate the quality of the regenerating tissue and the response to DCM transplantation. Table 3 summarizes the scores of seven previously defined criteria by Stoll [12] such as extracellular matrix (ECM) organization, cell/matrix ratio, cell distribution, organization of repair tissue, degenerative changes/tissue metaplasia, vascularization and inflammation. An intact Achilles tendon without any surgical operation was scored 12 points. Micrographs from all sections were captured at the suture regions (Leica DFC 420 by Leica Application Suite, V3.0).

2.9. Biomechanical analysis

Left Achilles tendons collected from the rats were sacrificed on postoperative weeks 4, 8, 12 and 24 and immediately wrapped in PBS-soaked gauze pads and kept at room temperature until testing (within 1 h of collection). Tendons were subjected to tensile testing (n = 5 for each time point) where gastrocnemius muscle and the calcaneus bone were fixed at each clamp of the universal testing machine (Instron 3367 with 100N load cell, Needham, MA). The length between the clamps was set at 5 mm and the samples were tested at 1 mm/s constant speed until failure. Maximum load, area, stiffness, ultimate tensile stress, extension at break, Young's Modulus, fracture strain, and energy uptake values were calculated for each sample. After mechanical testing, the samples were fixed in formaldehyde and embedded in paraffin blocks. Hematoxylene & Eosin stained histological slides were used to calculate the area of each sample. From each slide, low–magnification micrographs (4×) were captured (Leica DFC 420 by Leica Application Suite, V3.0) and then uploaded to Image J software. The area of each tendon section was calculated by plotting the outline boundary of width at the largest point and thickness manually in accordance with the literature to calculate the area of an irregular tissue [43–46].

Table 2
Summary of experimental groups.

Condition	Description
Control Group (n = 30)	Implantation of autologous tendon
DCM − Control Group (n = 30)	Implantation of allogeneic tendon
DCM + Tenocyte Group (n = 30)	Implantation of allogeneic tendon seeded with tenocytes

Table 3
Histological scoring system.

Histological criteria	Points
Extracellular matrix (ECM) organization	
Wavy, compact and parallel arranged collagen fibers	2
In part compact, in part loose collagen fibers	1
Loosely composed collagen fibers with granulation tissue	0
Cell/matrix ratio	
Physiological	2
Locally increased cell density	1
Increased cell density	0
Cell distribution	
Homogeneous and physiological	1
Heterogeneous and cell clustering	0
Organization of repair tissue	
Homogeneous	2
Locally heterogeneous	1
Whole tissue composition changed	0
Degenerative changes/tissue metaplasia	
Non existing	3
Moderate formation of edema	2
Intense edema and gap formation	1
Assembly of cartilage or bone	0
Vascularization	
Hypo − vascularized	1
Hyper − vascularized	0
Inflammation	
No inflammatory cells	1
Inflammatory cell types (neutrophils, macrophages and giant cells)	0
Max total	**12**

2.10. Statistical analysis

Statistical analyses of qRT-PCR, histopathological scoring and biomechanical testing were performed with one-way ANOVA and *post-hoc* Bonferroni tests by Statistica Software (V8.0). Statistical significance was assigned at $p \leq 0.05$ level.

3. Results

3.1. Tenocyte culture, proliferation and senescence

In explant culture, tenocytes started to migrate through the plate surface on day 10 (Fig. 1A, B). The average time to reach confluency was 4 days. All tenocytes exhibited elongated nuclei and spindle-shaped characteristic cytoplasm (Fig. 1C, D). All three passages (P1, P2 and P3) showed similar growth curves (Fig. 2) and cells grew exponentially without a lag phase during first few days and reached confluency by day 5 on T25 flask, after which cell viabilities started to decrease.

Primary tenocytes (P0) were used as control for β-galactosidase activity (Fig. 3A) and no staining was observed as these cells are not senescent. However, cellular senescence was observed in all passages and it kept increasing with an increasing passage number, which is measured counting the cells stained positively for β-galactosidase (Fig. 3B, C, D).

3.2. Immunofluorescence staining

All three passages (P1, P2, P3) showed strong staining with collagen type I, II, III, V, tenomodulin and tenascin-C (Fig. 4)

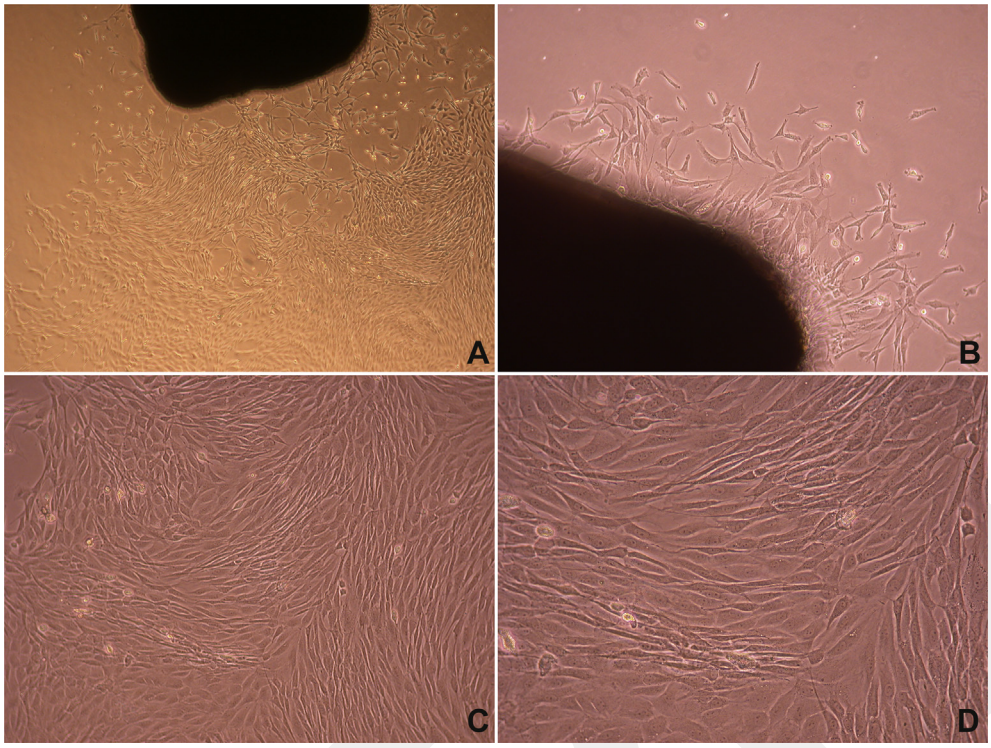

Fig. 1. The primary A. (×40), B. (×100) and secondary cultures, C. (×100), D. (×200) of tenocytes.

antibodies. Compared to these, as expected, collagen type II showed a much milder staining, which can be attributed to collagen type II as a major marker of cartilage tissue and it is also reported to be present in tenocyte cytoplasm [45].

3.3. Gene expression analysis with qPCR

The results were compared between P1–P2, P2–P3 and P1–P3 samples. Gene expressions were observed to be significantly affected by passage number ($p < 0.05$) (Fig. 5).

Except for *Tnsc*, all qPCR results indicated significantly increased target gene amplifications in P2 and P3, over P1 ($p < 0.05$). The increase in the expression of target genes (*Col I, Col II, Col III, Col V, Tnmd* and *Tnsc*) was less in P2 when compared with P3. On the contrary, expression of *Tnsc* relative to *Gapdh* was decreased through P1 to P3. As a chondrogenic lineage marker (negative control), *Col II* gene expression relative to *Gapdh* started at very late PCR cycles (~40), which indicates that the expression of *Col II* is relatively lower compared with the other target genes.

3.4. Histology of in vitro engineered and in vivo remodeled tendons

Regardless of the transplanted graft type, general appearance of the tendons was similar in all rats at the end of study: They all showed macroscopic characteristics of intact tendons but with tissue edema commonly observed due to higher sulfated proteoglycan content which is responsible for water-binding [14]. Thickness of the tendons appeared to decrease with healing over time. The seeded tendon grafts were histologically indistinguishable in all experimental groups. Both DCM and DCM + tenocyte constructs regained normal collagen architecture 12 weeks after surgery.

The histological scores and histopathological findings are given in Figs. 6 and 7, respectively. At every time point, intact tendon and each one of the experimental groups showed statistically significant differences in their histological scores for each evaluated histological criteria ($p < 0.05$). Within each specific criterion at every study week, at the end of the 24th week, DCM + Tenocyte group obtained the highest scores ($p < 0.05$) among all the tested groups, indicating that this group exhibited the most successful tendon structural recovery.

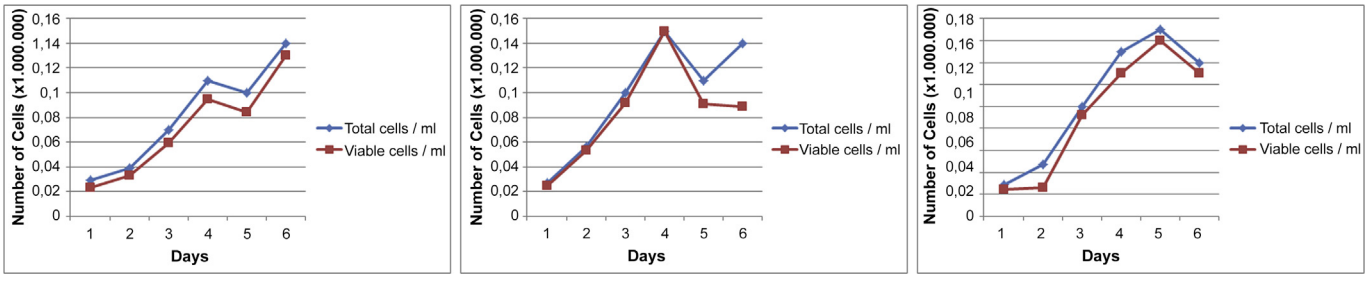

Fig. 2. Growth curves of P1, P2 and P3 tenocytes by means of total cell/mL and viable cells/mL.

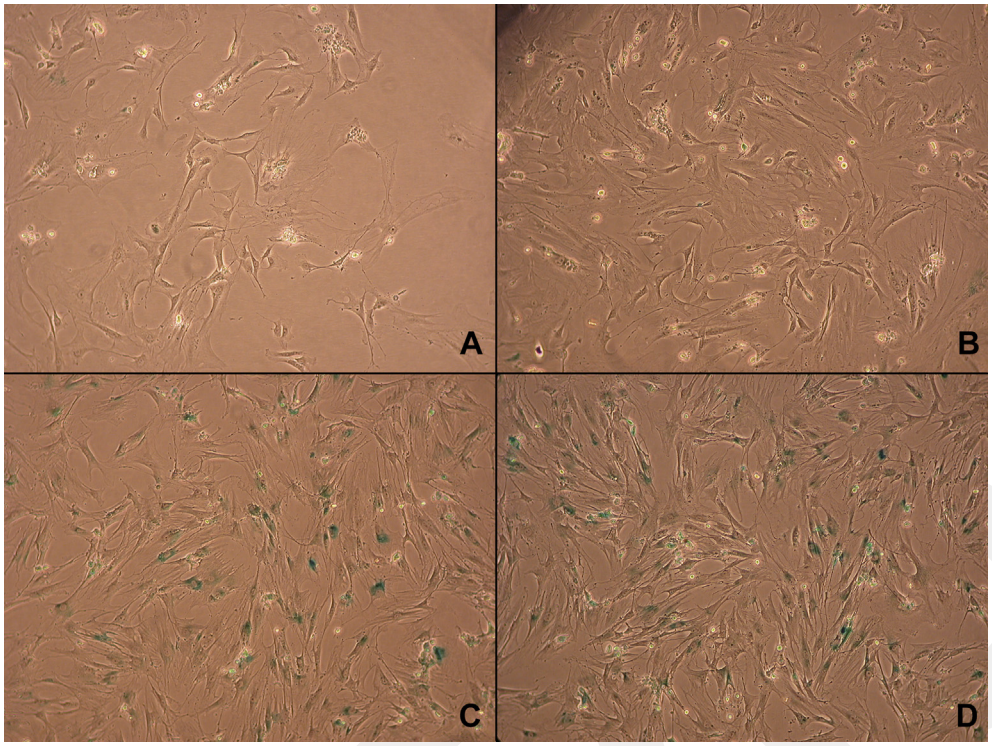

Fig. 3. β-galactosidase activity of A. P0 (×100), B. P1 (×100), C. P2 (×100) and D. P3 (×100) tenocytes. The blue stained cells indicate positive β-galactosidase activity. (For interpretation of the references to color in this figure legend, the reader is referred to the web version of this article.)

In comparison with non-operated normal tendon and the experimental groups, a higher degree of inflammation was evident in all operated groups with visible neutrophils and phagocytic cells in all experimental groups (Fig. 7 A–C). Giant cells were detected mostly around sutures in all groups (Fig. 7 J–L). However, DCM − Tenocyte group had less inflammatory cells than Control and DCM − Control groups ($p < 0.05$), indicating a higher degree of tendon callus organization with more extensive regeneration.

Cell/matrix ratio and vascularization were similar in all groups throughout the study. According to histopathological examination results, during the first inflammatory phase of healing, all groups had focal cell accumulations and increased cellular density with a hypervascularized structure (Fig. 7 M–O). There were no significant differences by means of cell/matrix ratio and vascularization among groups ($p > 0.05$). However, cell distribution was more homogeneous and the number of cells was closer to physiological distribution in DCM + Tenocyte group when compared with Control and DCM − Control groups ($p < 0.05$).

Compared with the Control and DCM − Control groups, DCM + Tenocyte groups showed a significantly better organized ECM with the collagen fibers being compact and aligned in parallel to each other (Fig. 7 G–I, S–U), indicative of a more successful organization of the repair tissue in DCM + Tenocyte group. The structure of ECM and the general surrounding tissue structure were more homogeneous in DCM + Tenocyte group when compared with Control and DCM − Control ($p < 0.05$).

Degenerative changes/tissue metaplasia were detected in all experimental groups (Fig. 7 P–R). However, in DCM + Tenocyte group, these changes were statistically fewer than Control and DCM − Control groups. Out of 90 animals, 15, 21, and 12 animals developed chondroid metaplasia in the control, DCM − Control, and DCM + Tenocyte group, (representing 16.6%, 23.3%, and 13.3% of all cases within the groups), respectively. In DCM + Tenocyte group, only 2 of the 90 animals (2.2%) developed gap formation whereas it was not observed in any of the animals in other groups. Bonferroni test results suggested that presence of chondroid metaplasia was statistically lower in DCM + Tenocyte group ($p < 0.05$) and the rate of gap formation was not significantly different between the experimental groups ($p > 0.05$). The histologic appearance of native tendon tissue at 24 week is given in Fig. 8.

3.5. Biomechanical test results

All specimens were successfully tested without any specimen lost. Mechanical test results, shown in Table 4, suggest that the repair in DCM + Tenocyte group over time was the best in all groups. The improvement of ultimate tensile stress (UTS) values in DCM + Tenocyte group were significantly higher than other groups at each postoperative time point tested ($p < 0.05$). Furthermore, postoperative tendon cross sectional area values for DCM + Tenocyte group were lower than those of Control groups in most of the time points. These two observations suggest that DCM + Tenocyte grafting provides a faster tendon remodeling in this model. The results also demonstrate that both DCM − Control and DCM + Tenocyte groups showed similar patterns during tensile tests, indicating a correlating regeneration process. The stiffness at all postoperative weeks with the exception of the 4th week, increased with time and DCM application ($p < 0.05$). The energy uptake of DCM + Tenocyte group showed an increase in all postoperative weeks. However, only the data obtained from postoperative 4th week was significantly higher ($p < 0.05$) when compared with Control group.

Postoperative Young's Modulus data for all groups increased at all-time points and they all reached to similar values at the end of the 24th week. However, the ultimate values of Young's modulus were obtained at 12th weeks in DCM + control groups while they were reached only at 24th weeks in the other two groups. This fact also suggests that a faster tissue remodeling process occurred in the DCM + Tenocyte group tendons.

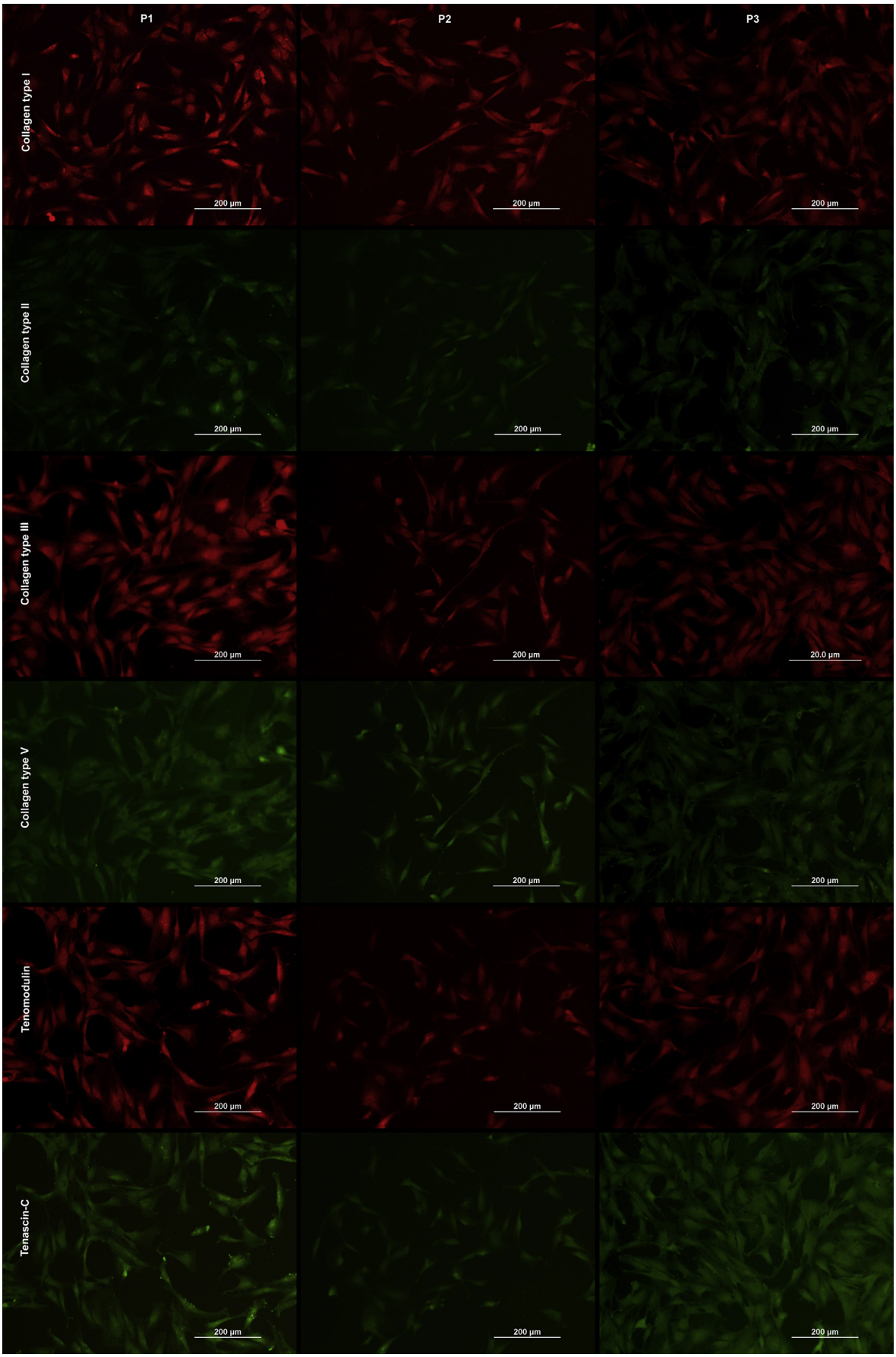

Fig. 4. Immunofluorescence staining results of P1, P2 and P3 tenocytes with collagen type I/II/III/V, tenomodulin and tenascin − C antibodies. Texas Red and FITC were used as red and green fluorochromes respectively. (For interpretation of the references to color in this figure legend, the reader is referred to the web version of this article.)

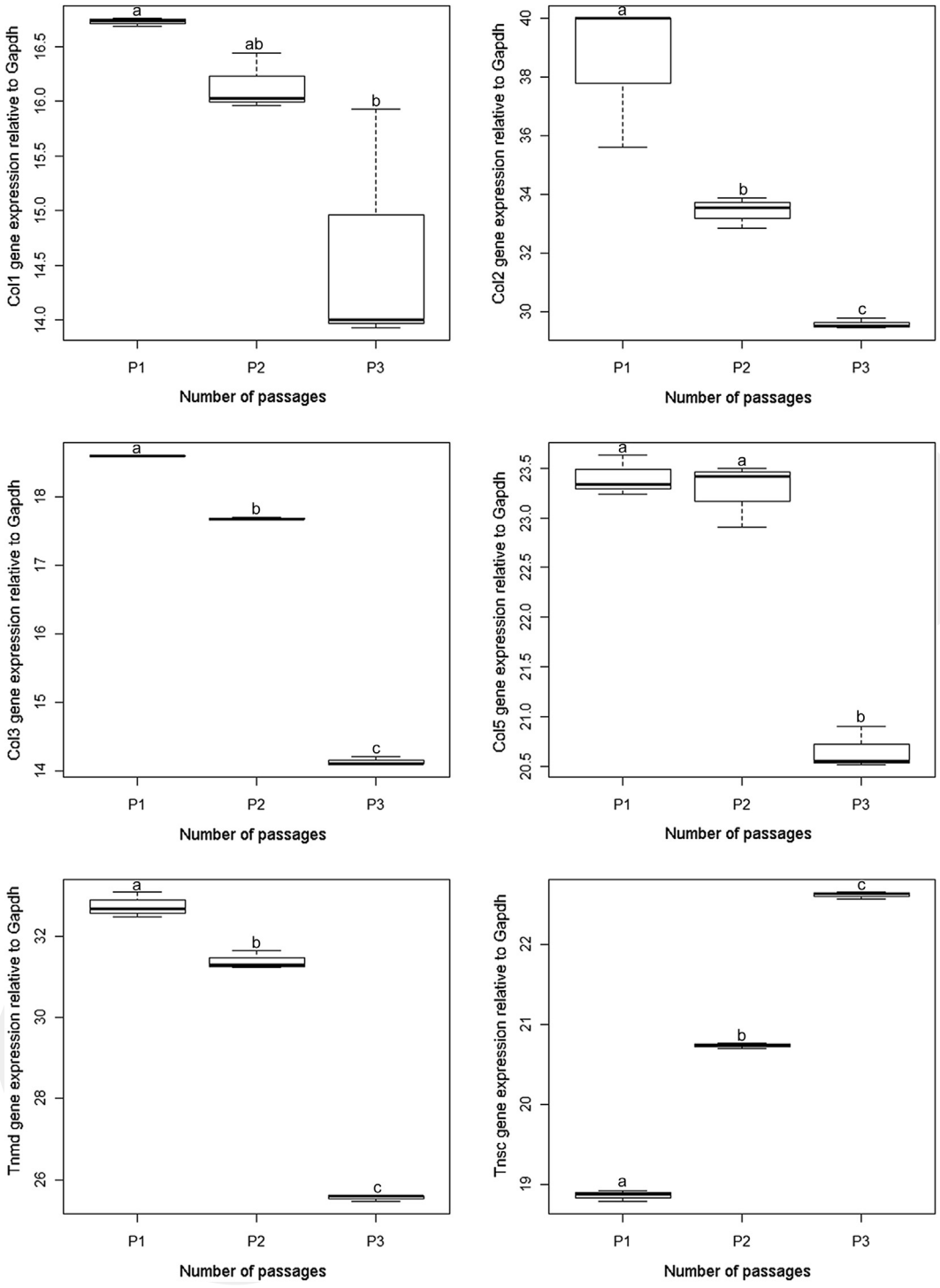

Fig. 5. Real-time quantitative-polymerase chain reaction results of collagen type I (*Col1*), collagen type II (*Col2*), collagen type III (*Col3*), collagen type V (*Col5*), tenomodulin (*Tnmd*) and tenascin − C (*Tnsc*) in P1, P2 and P3 tenocytes. In each figure, x-axis indicates the number of passages as P1, P2, P3 and y-axis indicates each gene's expression ratio (Mean C_T) relative to glyceraldehyde-3-phosphate dehydrogenase (*Gapdh*).

4. Discussion

The objective of the present study was to examine the regenerative effect of DCM + Tenocyte composites on Achilles tendon regeneration. To achieve this, DCM + Tenocyte composites were implanted in Achilles tendons of rats with tendon defect and the results were examined by means of histological and biomechanical alterations that occurred throughout 24 weeks. Implantation of DCM + Tenocyte composites considerably enhanced and speeded up Achilles tendon regeneration.

Since tenocytes exhibit a low proliferative capacity under *in vitro* conditions, we first examined the proliferation ability of tenocytes prior to seeding on DCM and found that tenocytes have grown successfully in monolayer culture. Tenocytes were also screened for β-galactosidase activity and all passages indicated mild cellular senescence except primary culture (P0), which did not

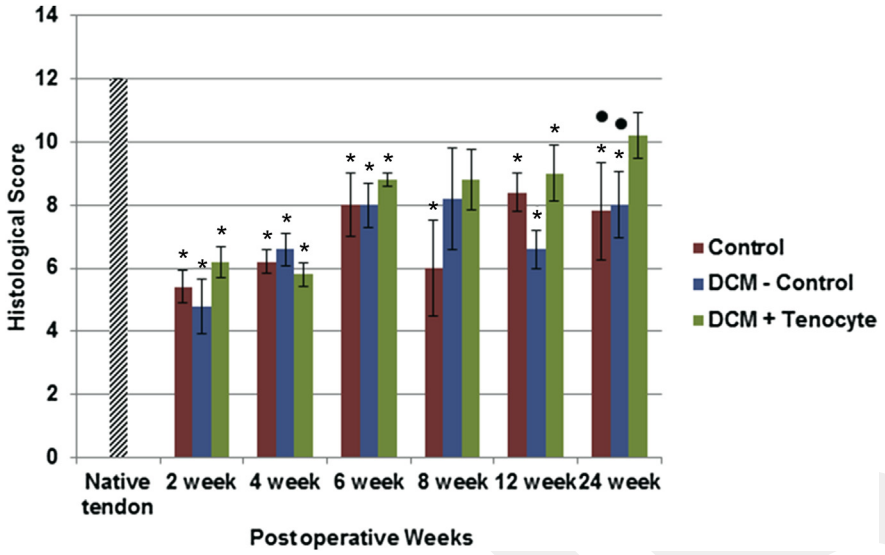

Fig. 6. Results of histological scoring of native and repaired tendons at 2nd, 4th, 6th, 8th, 12th and 24th postoperative weeks in Control, DCM − Control and DCM + Tenocyte groups (n = 5 for each group). All specimens were compared to untreated native tendon (*p < 0.05: significantly different from native tendon score and •p < 0.05: significantly different from DCM + Tenocyte group).

indicate senescence. This is in accordance with the observation that tenocytes originating from rabbit tendon maintain their viability without any sign of senescence [1]. To more precisely determine whether a mild senescence would affect *in vitro* characteristics, we performed immunofluorescence staining and qPCR for the presence and expression of several markers that mediate the growth and repair of the tendon. Pauly [47] reported that collagen type I and type III cannot be considered alone as tenocyte markers. In the current study, immunofluorescence staining results showed that collagen type I, III, V, tenomodulin and tenascin-C were detected in tenocytes of different passages (P1, P2, P3). These molecules were previously reported as tendon specific proteins [48,49]. Other authors suggested that moderate collagen type II expression is also present in human tenocytes [50,51]. Due to low levels of collagen type II detected, our results are consistent with these findings. The expressions of other molecules also exhibited a similar distribution in qPCR. Lou [49] reported that the increased expression of *Col1* together with *Col3* is the indicator for tenocyte differentiation. In addition, *Tnsc* as a trauma marker decreased over the course of passaging which indicated that the tenocytes retrained their capacity to proliferate without any stress under *in vitro* conditions of present study. This result is consistent with Pauly [47] who reported that *Tnsc* expression is elevated in degenerative tendon and it is specifically elevated in chondrocytes and osteoblasts. Jelinsky [52] claimed *Tnmd* as a specific protein with a high expression in tendon compared to other tissues, which is a likely case seen in our results. These findings suggested that there is no phenotypic or genotypic drift in tenocytes to be reseeded on tendon constructs.

Several approaches to establish DCM for tendon reconstruction were discussed by Woods and Gratzer [53]. The main problem in DCM application is the rejection of the graft material by immune response and the inadequacy of the graft while the regenerating tendon gains it histologic/biomechanical properties. To overcome this problem, Triton X − 100 and SDS were used as decellularization agents in the current study to obtain DCM, in accordance with the recommendations of Woods and Gratzer [53]. Our results confirmed the effectiveness of this protocol for the removal of cellular material of tendon tissue.

Tendon healing is characterized in three consequent stages: i. inflammatory phase, ii. fibroblastic phase, and iii. remodeling phase [54–56]. During the inflammatory phase, which lasts about 1–2 weeks, the granulation tissue formed by the migration of fibroblastic and inflammatory cells accompanied by hypervascularization is observed in healing zone. Analogously, we observed the formation of the granulation tissue in all groups at postoperative 2 and 4 weeks. During the fibroblastic phase, which lasts about 3–6 weeks, the proliferation of fibroblasts, collagen and other ECM components is evident in healing zone [43]. Consistent with this finding, the accumulation of fibroblasts and loosely composed collagen fibers were detected at postoperative 6 and 8 weeks. The remodeling phase consists of parallel organization of the newly synthesized collagen fibers accompanied by a reduction observed in cell/matrix ratio [54]. In accordance, at postoperative 12 and 24 weeks, compact parallel arrangement of collagen fibers and physiologically normal cell/matrix ratio were evident in the current study.

Chondroid metaplasia is the fibrous cartilage formation at osteotendinous junction and we observed chondroid metaplasia in the tendons of all groups, at all postoperative weeks. Moreover, the severity of chondroid metaplasia in DCM + Tenocyte group was significantly lower than Control and DCM − Control groups. Recent studies suggest that chondroid metaplasia is formed in response to a lack of tensile load [57]. A lower severity of chondroid metaplasia in DCM + Tenocyte group observed in this study indicates a higher extent of tensile loading applied on the regenerating tendon tissue. This situation can be explained so as the regeneration process in DCM + Tenocyte group was more successful and took place earlier. This might have allowed the animals in this group to regain their physical activity in the earlier stages of healing, letting them apply more load to their legs to cause a less severe chondroid metaplasia in their tendons.

Compared to Control and DCM − Control Group, the histopathological results of the DCM + Tenocyte group indicated a better healing response with a more successful matrix organization, more homogeneous cell distribution and a more successful repair tissue organization throughout the healing period.

According to previous studies, the biomechanical properties of healing tendon change during recovery period as well as histological characteristics. Therefore, the assessment of biomechanical properties is also of prime importance to evaluate the success of the applied technique for tendon regeneration [58]. Whitlock [34] reported that scaffolds composed of collagen do not produce any harmful degradation products as synthetic

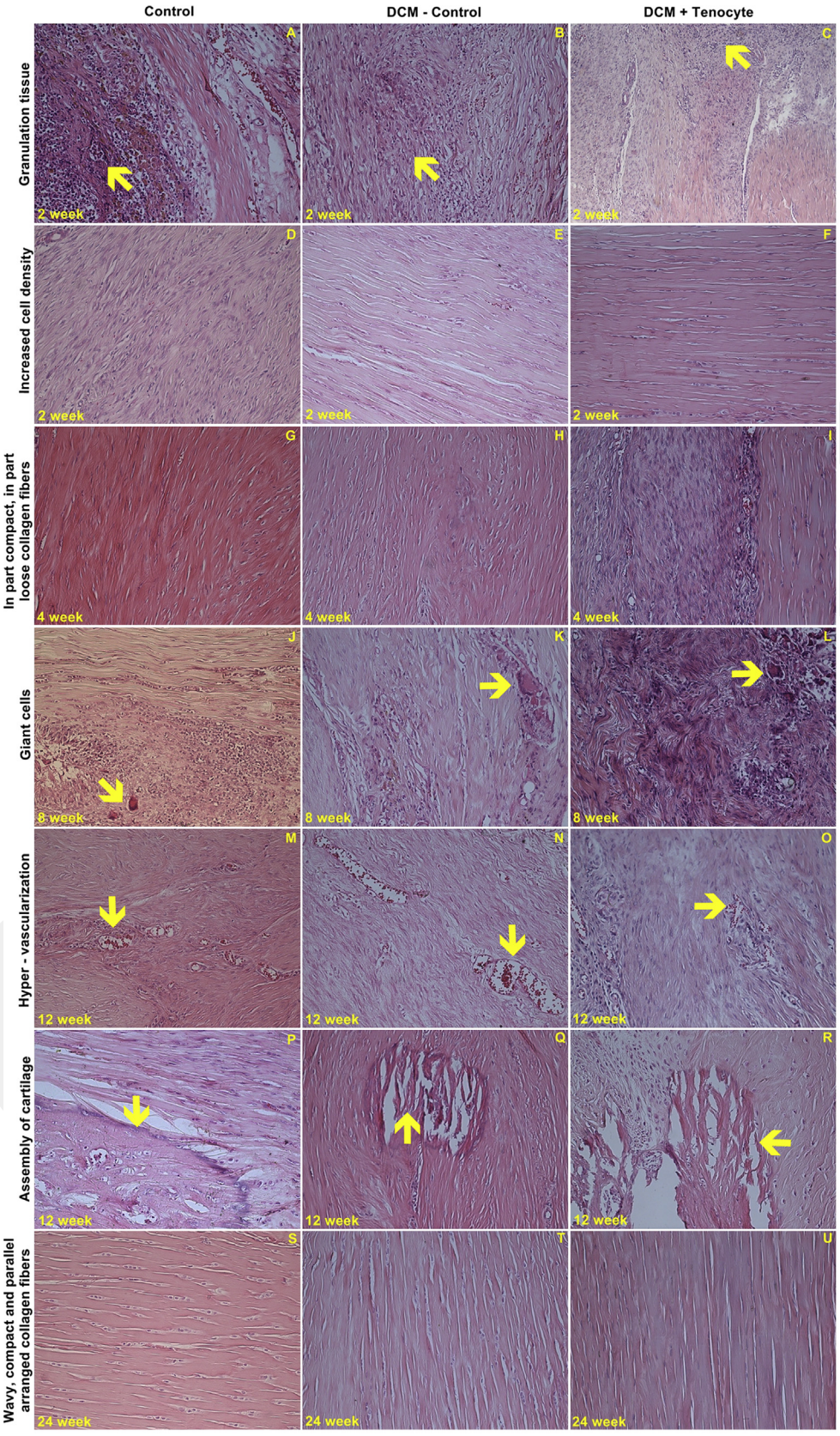

Fig. 7. Histopathological findings of repaired tendons at 2nd, 4th, 6th, 8th, 12th and 24th postoperative weeks in Control, DCM − Control and DCM + Tenocyte groups. Pathological examinations were based on H&E stained 5 μm-thick longitudinal sections of tendons in each group (×100). Yellow arrows indicate the granulation tissue (A/B/C), giant cells (J/K/L), hyper − vascularization (M/N/O) and chondroid metaplasia (P/Q/R) respectively. (For interpretation of the references to color in this figure legend, the reader is referred to the web version of this article.)

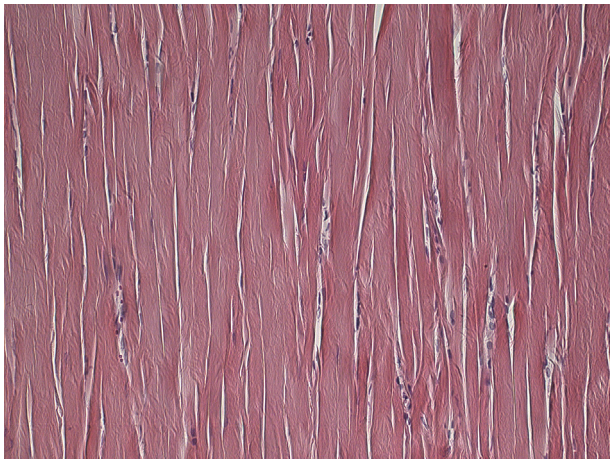

Fig. 8. The histological appearance of native tendon tissue at 24 week (H&E staining, ×100).

polymers and these scaffolds have better capability to enhance regeneration by promoting a stronger adhesion surface for tenocytes. Thus, the increase in histologic organization during tendon healing suggests an expectation of better biomechanical properties. Reddy [59] suggested that the production of collagen matrix is directly associated with the tensile strength of tendon. According to our biomechanical results, maximum load, stiffness, ultimate tensile stress, energy uptake and Young's modulus of elasticity were low, which is consistent with less tissue organization during the early weeks. Furthermore, the cross sectional area of tendons in the Control group animals was the highest at all postoperative weeks; indicative of a more persistent tendon callus due to slow and limited matrix organization and decreased mechanical properties. This result is coherent with Perry [44] who obtained similar results after applying small intestine submucosa in a rat model for tendon repair. The similar ultimate tensile stress patterns in both DCM − Control and DCM + Tenocyte groups obtained in the current study can be explained by the fact that tendon is a sturdy tissue and it is not mechanically degenerated easily even after decellularization process. This finding is consistent with the findings of Whitlock [34] who presented that decellularized tendon grafts promote regeneration process while retaining the majority of the tensile properties of the tissue. Therefore, both DCM − Control and DCM + Tenocyte groups reflected this expectation. Also, in both groups, the fracture strain values continued to increase with the time passed, suggesting occurrence of tissue remodeling. The corresponding material properties: fracture strain energy to maximum stress and ultimate tensile stress − Young's modulus to postoperative weeks were also monitored for all groups. In the analysis of all groups together, DCM + Tenocyte group was the most successful in withstanding loading force and the mechanical properties such as ultimate tensile stress and Young's modulus were increased by DCM + Tenocyte treatment. These findings from current study support our hypothesis that allografting tissue engineered DCM scaffolds with tenocytes provides a significantly faster healing in rats − compared to both non-tissue engineered DCM and non-grafted control groups − which was supported by the observations of better histologic and mechanical properties.

Tissue engineering approaches should provide the development of new graft materials which enhance the regeneration period with minimum postoperative complications. Differently from other studies, the current study demonstrated the feasibility of generating a naturally derived scaffold material with previously characterized tenocytes which provides a successful substrate for enhancing the recovery period. Decellularized matrices and these matrices together with seeded cells as scaffolds assure to enhance healing without causing immune response by the patient. Due to the difficulty of the surgical procedure that needs to be applied to the small area, the rat Achilles tendon is not a frequently preferred repair model. However, this study showed that it is a feasible model especially for long term *in vivo* tendon healing studies.

5. Conclusions

In recent study, tenocyte seeded DCM was proved to improve Achilles tendon regeneration process in rats by both histological and biomechanical means. DCM + Tenocyte composites did not cause any immune response and speeded up the regeneration process of Achilles tendon. In rats with Achilles tendon defects, a better ECM organization, physiological cell/matrix ratio, and homogeneous cell distribution were correlated with increased ultimate tensile stress and fracture strain due to DCM + Tenocyte composite's implantation. To our knowledge, this is the first long term study in the literature which was accomplished in a model of rat Achilles tendon. Although the rat Achilles tendon model used in this study does not fully match the condition in humans, the method developed in this study might have important implications for translation into the clinic. In addition, it would also be suggested that the use of rat model is both feasible and cost effective to study tendon regeneration.

Table 4
Mechanical testing results.

Groups		Maximum load (N)	Area (mm2)	Ultimate tensile stress (MPa)	Extension at break (mm)	Stiffness (%)	Energy uptake (mJ)	Fracture strain (%)	Young's Modulus (MPa)
4 week	Control	39.11 ± 4.35[b,c]	19.34 ± 0.47[c]	2.01 ± 0.19[b,c]	1.44 ± 0.19[c]	29.26 ± 5.39	57.02 ± 11.67[b,c]	0.31 ± 0.26[b,c]	11.45 ± 0.64
	DCM-Control	62.57 ± 3.22[a]	16.78 ± 0.77	3.75 ± 0.23[a]	3.06 ± 0.59	23.60 ± 4.16	186.41 ± 20.67[a]	0.53 ± 0.56[a]	12.00 ± 1.85
	DCM + Tenocyte	60.52 ± 1.77[a]	14.87 ± 0.73[a]	4.10 ± 0.19[a]	3.18 ± 0.45[a]	21.23 ± 4.26	190.59 ± 24.54[a]	0.64 ± 0.01[a]	11.00 ± 1.70
8 week	Control	51.93 ± 2.40[c]	19.4 ± 0.93[b]	2.71 ± 0.20[b,c]	2.43 ± 0.42	23.44 ± 3.20[c]	128.43 ± 25.40	0.42 ± 0.04	9.37 ± 0.69
	DCM-Control	49.14 ± 2.66[c]	17.30 ± 0.53[a,c]	3.75 ± 0.19[a]	1.90 ± 0.13	26.34 ± 2.27[c]	93.19 ± 6.66	0.38 ± 0.03	12.34 ± 0.42
	DCM + Tenocyte	71.89 ± 2.79[a,b]	19.89 ± 1.44[b]	3.66 ± 0.19[a]	1.84 ± 0.18	40.39 ± 3.68[a,b]	131.88 ± 12.48	0.37 ± 0.04	11.11 ± 1.16
12 week	Control	81.24 ± 2.69[b]	25.87 ± 0.94	3.17 ± 0.20	3.44 ± 0.45[b,c]	24.82 ± 2.38[c]	133.74 ± 46.11	0.60 ± 0.04[b,c]	8.26 ± 0.36[c]
	DCM-Control	61.86 ± 2.22[a,c]	21.67 ± 0.85	2.86 ± 0.05[c]	1.94 ± 0.23[a]	34.09 ± 4.96	120.20 ± 15.30	0.42 ± 0.03[a]	10.96 ± 0.62[c]
	DCM + Tenocyte	84.60 ± 2.90[b]	21.09 ± 2.12	5.17 ± 0.41[a,b]	1.98 ± 0.19[a]	44.32 ± 4.12[a]	167.35 ± 16.61	0.42 ± 0.03[a]	15.36 ± 1.28[a,b]
24 week	Control	78.89 ± 4.05[c]	19.68 ± 1.61	4.08 ± 0.60[c]	3.79 ± 1.02	27.63 ± 6.36	297.08 ± 77.03	0.56 ± 0.08	14.25 ± 1.10
	DCM-Control	89.91 ± 2.93	18.62 ± 0.84	4.87 ± 0.24[c]	2.43 ± 0.60	51.48 ± 16.69	221.10 ± 58.20	0.49 ± 0.06	15.00 ± 2.67
	DCM + Tenocyte	99.61 ± 3.08[a]	15.66 ± 1.07	6.38 ± 0.32[a,b]	3.10 ± 0.53	54.94 ± 4.28[a]	314.83 ± 59.86	0.60 ± 0.01	15.60 ± 0.70

[a] $p < 0.05$ significantly different from Control Group.
[b] $p < 0.05$ significantly different from DCM − Control Group.
[c] $p < 0.05$ significantly different from DCM + Tenocyte Group.

Acknowledgments

This study was conducted within the scope of the PhD thesis of Cansın Güngörmüş. Financial support for the conduct of this work was provided by The Scientific and Technological Research Council of Turkey (TUBITAK, Project Number: 109T977) under a research project grant to Hacettepe University Department of Biology. Authors would like to thank Dr. Aykut Özkul, Dr. Hilal Özdağ, Dr. M. Alper Çetinkaya, and Dr. Aslı Korkmaz for their valuable suggestions to this study.

References

[1] Bernard-Beaubois K, Hecquet C, Houcine O, Hayem G, Adolphe M. Culture and characterization of juvenile rabbit tenocytes. Cell Biol Toxicol 1997;13:103–13.
[2] Kannus P. Structure of tendon connective tissue. Scand J Med Sci Sports 2000;10:312–20.
[3] Rees SG, Flannery CR, Little CB, Hughes CE, Caterson B, Dent CM. Catabolism of aggrecan, decorin and biglycan in tendon. Biochem J 2000;350:180–8.
[4] Leppilahti J, Puranen J, Orava S. Incidence of Achilles tendon rupture. Acta Orthop Scand 1996;67:277–9.
[5] Clayton RAE, Court-Brown CM. The epidemiology of musculoskeletal tendinous and ligamentous injuries. Injury 2008;39:1338–44.
[6] Shearn JT, Kinneberg KRC, Dyment NA, Galloway MT, Kenter K, Wylie C, et al. Tendon tissue engineering: progress, challenges, and translation to the clinic. J Musculoskelet Neuronal Interact 2011;11:163–73.
[7] Rotini R, Fini M, Giavaresi G, Marinelli A, Guerra E, Antonioli D, et al. New perspectives in rotator cuff tendon regeneration: review of tissue engineered therapies. Chir Organ Mov 2008;91:87–92.
[8] Quyang HW, Goh JC, Thambyah A, Teoh SH, Lee EH. Knitted poly-lactide-co-glycolide scaffold loaded with bone marrow stromal cells in repair and regeneration of rabbit Achilles tendon. Tissue Eng 2003;9:431–9.
[9] Juncosa-Melvin N, Boivin GP, Galloway MT, Gooch C, West JR, Butler DL. Effects of cell-to-collagen ratio in stem cell-seeded constructs for Achilles tendon repair. Tissue Eng 2006;2:681–9.
[10] Liu Y, Ramanath HS, Wang DA. Tendon tissue engineering using scaffold enhancing strategies. Trends Biotechnol 2008;26:201–9.
[11] Stoll C, John T, Endres M, Rosen C, Kaps C, Kohl B, et al. Extracellular matrix expression of human tenocytes in three-dimensional air-liquid and PLGA cultures compared with tendon tissue. J Orthop Res 2010;28:1170–7.
[12] Stoll C, John T, Conrad C, Lohan A, Hondke S, Ertel W, et al. Healing parameters in a rabbit partial tendon defect following tenocyte/biomaterial implantation. Biomaterials 2011;32:4806–15.
[13] Bagnaninchi PO, Yang Y, El Haj AJ, Maffulli N. Tissue engineering for tendon repair. Br J Sports Med 2007;41:1–5.
[14] Sharma B, Elisseeff JH. Engineering structurally organized cartilage and bone tissues. Ann Biomed Eng 2004;32:148–59.
[15] Cao Y, Liu Y, Liu W, Shan Q, Buonocore SD, Cui L. Bridging tendon defects using autologous tenocyte engineered tendon in a hen model. Plast Reconstr Surg 2002;110:1280–9.
[16] Quyang HW, Goh JC, Mo XM, Teoh SH, Lee EH. The efficacy of bone marrow stromal cell-seeded knitted PLGA fiber scaffold for Achilles tendon repair. Ann N Y Acad Sci 2002;961:126–9.
[17] Funakoshi T, Majima T, Suenaga N, Iwasaki N, Yamane S, Minami A. Rotator cuff regeneration using chitin fabric as an acellular matrix. J Shoulder Elbow Surg 2006;15:112–8.
[18] Reverchon E, Baldino L, Cardea S, De Marco I. Biodegradable synthetic scaffolds for tendon regeneration. Muscles Ligaments Tendons J 2012;2:181–6.
[19] Hildebrand KA, Frank CB, Hart DA. Gene intervention in ligament and tendon: current status, challenges, future directions. Gene Ther 2004;11:368–78.
[20] Hankemeier S, Keus M, Zeichen J, Jagodzinski M, Barkhausen T, Bosch U, et al. Modulation of proliferation and differentiation of human bone marrow stromal cells by fibroblast growth factor 2: potential implications for tissue engineering of tendons and ligaments. Tissue Eng 2005;11:41–9.
[21] Doroski DM, Levenston ME, Temenoff JS. Cyclic tensile culture promotes fibroblastic differentiation of marrow stromal cells encapsulated in poly(ethylene glycol)-based hydrogels. Tissue Eng Part A 2010;16:3457–66.
[22] Awad HA, Butler DL, Boivin GP, Smith FN, Malaviya P, Huibregtse B, et al. Autologous mesenchymal stem cell-mediated repair of tendon. Tissue Eng 1999;5:267–77.
[23] Stein L. Effects of serum, fibroblast growth factor and platelet-derived growth factor on explants of rat tail tendon: a morphological study. Acta Anat 1985;123:247–53.
[24] Chan BP, Chan KM, Maffulli N, Webb S, Lee KK. Effect of basic fibroblast growth factor; an in vitro study of tendon healing. Clin Orthop Relat Res 1997;342:239–47.
[25] Chan BP, Fu S, Qin L, Lee K, Rolf CG, Chan K. Effects of basic fibroblast growth factor (bFGF) on early stages of tendon healing: a rat patellar tendon model. Acta Orthop 2000;71:513–8.
[26] Jørgensen H, McLellan SD, Crossan JF, Curtis ASG. Neutralization of TGF [beta] or binding of VLA-4 to fibronectin prevents rat tendon adhesion following transection. Cytokine 2005;30:195–202.
[27] Bonadio J. Tissue engineering via local gene delivery: update and future prospects for enhancing the technology. Adv Drug Deliv Rev 2000;44:185–94.
[28] Huang D, Balian G, Chhabra A. Tendon tissue engineering and gene transfer: the future of surgical treatment. J Hand Surg Am 2006;31:693–704.
[29] Cotrim AP, Baum BJ. Gene therapy: some history, applications, problems and prospects. Toxicol Pathol 2008;36:97–103.
[30] Huang D, Balian G, Chhabra B. Tendon tissue engineering and gene transfer: the future of surgical treatment. J Hand Surg 2006;31A:693–704.
[31] Derwin KA, Badylak SF, Steinmann SP, Iannotti JP. Extracellular matrix scaffold devices for rotator cuff repair. J Shoulder Elbow Surg 2010;19:467–76.
[32] Fini M, Bandioli E, Castagna A, Torricelli P, Giavaresi G, Rotini R, et al. Decellularized human dermis to treat massive rotator cuff tears: in vitro evaluations. Connect Tissue Res 2012;53:298–306.
[33] Ricchetti ET, Aurora A, Iannotti JP, Derwin KA. Scaffold devices for rotator cuff repair. J Shoulder Elbow Surg 2012;21:251–65.
[34] Whitlock PW, Smith TL, Poehling GG, Shilt JS, Dyke MV. A naturally derived, cytocompatible and architecturally optimized scaffold for tendon and ligament regeneration. Biomaterials 2007;28:4321–9.
[35] Ott HC, Clippinger B, Conrad C, Schuetz C, Pomerantseva I, Ikonomou L, et al. Regeneration and orthotopic transplantation of bioartificial lung. Nat Med 2010;16:927–33.
[36] Uygun BE, Soto-Gutierrez A, Yagi H, Izamis ML, Guzzardi MA, Shulman C, et al. Organ reengineering through development of a transplantable recellularized liver graft using decellularized liver matrix. Nat Med 2010;16:814–20.
[37] Liu Y, Wang L, Kikuiri T, Akiyama K, Chen C, Xu X. Mesenchymal stem cell-based tissue regeneration is governed by recipient T lymphocytes via IFN-gamma and TNF-alpha. Nat Med 2011;17:1594–601.
[38] Wu W, Allen RA, Wang Y. Fast-degrading elastomer enables rapid remodeling of a cell-free synthetic graft into a neoartery. Nat Med 2012;18:1148–53.
[39] Liu W, Chen B, Deng D, Xu F, Cui L, Cao Y. Repair of tendon defect with dermal fibroblast engineered tendon in a porcine model. Tissue Eng 2006;12:775–88.
[40] Güngörmüş C, Kolankaya D. Gene expression of tendon collagens and tenocyte markers in long-term monolayer and high-density cultures of rat tenocytes. Connect Tissue Res 2012;53:485–91.
[41] Pfaffle MW. A new mathematical model for relative quantification in real-time RT-PCR. Nucleic Acids Res 2001;29:e45.
[42] Güngörmüş C, Çetinkaya MA, Demirutku A. A new model for partial immobilization of rat hind limb after Achilles tendon excision/re-interposition. Turk J Vet Anim Sci 2013;37:546–52.
[43] Thomopoulos S, Soslowsky LJ, Flanagan CL, Tun S, Keefer CC, Mastaw J, et al. The effect of fibrin clot on healing rat supraspinatus tendon defects. J Shoulder Elbow Surg 2002;11:239–47.
[44] Perry SM, Gupta RR, Van Kleunen J, Ramsey ML, Soslowsky LJ, Glaser DL. Use of small intestine submucosa in a rat model of acute and chronic rotator cuff tear. J Shoulder Elbow Surg 2007;16:S179–83.
[45] Leung KS, Qin L, Fu LK, Chan CW. A comparative study of bone to bone repair and bone to tendon healing in patella–patellar tendon complex in rabbits. Clin Biomech 2002;7:594–602.
[46] Dejardin LM, Arnoczky SP, Ewers BJ, Haut RC, Clarke RB. Tissue-engineered rotator cuff tendon using porcine small intestine submucosa. Histologic and mechanical evaluation in dogs. Am J Sports Med 2001;29(2):175–84.
[47] Pauly S, Klatte F, Strobel C, Schmidmaier G, Greiner S, Scheibel M, et al. Characterization of tendon cell cultures of the human rotator cuff. Eur Cell Mater 2010;20:84–97.
[48] Docheva D, Hunziker EB, Fassler R, Brandau O. Tenomodulin is necessary for tenocytes proliferation and tendon maturation. Mol Cell Biol 2005;25:699–705.
[49] Lou Q, Song G, Song Y, Xu B, Qin J, Shi Y. Indirect co-culture with tenocytes promotes proliferation and mRNA expression of tendon/ligament related genes in rat bone marrow mesenchymal stem cells. Cytotechnology 2009;61:1–10.
[50] Gigante A, Marinelli M, Chillemi C, Greco F. Fibrous cartilage in the rotator cuff: a pathogenetic mechanism of tendon tear? J Shoulder Elbow Surg 2004;13:328–32.
[51] Martin JA, Mehr D, Pardubsky PD, Buckwalter JA. The role of tenascin-C in adaptation of tendons to compressive loading. Biorheology 2003;40:321–9.
[52] Jelinsky SA, Archambault J, Li L, Seeherman H. Tendon-selective genes identified from rat and human musculoskeletal tissues. J Orthop Res 2010;28:289–97.
[53] Woods T, Gratzer PF. Effectiveness of three extraction techniques in the development of a decellularized bone-anterior cruciate ligament-bone graft. Biomaterials 2005;26:7339–49.
[54] Beredjiklian PK. Biologic aspects of flexor tendon laceration and repair. J Bone Jt Surg Am 2003;85A:539–50.
[55] Hamada Y, Katoh S, Hibino N, Kosaka H, Hamada D, Yasui N. Effects of monofilament nylon coated with basic fibroblast growth factor on endogenous intrasynovial flexor tendon healing. J Hand Surg Am 2006;31A:530–40.
[56] Matthews TJW, Hand GC, Rees JL, Athanasou NA, Carr AJ. Pathology of the torn rotator cuff tendon. Reduction in potential for repair as tear size increases. J Bone Jt Surg Br 2006;88B:489–95.
[57] Longo UG, Franceschi F, Ruzzini L, Rabitti C, Morini S, Maffuli N, et al. Light microscopic histology of supraspinatus tendon ruptures. Knee Surg Sports Traumatol Arthrosc 2007;15:1390–4.
[58] Nagasawa K, Noguchi M, Ikoma K, Kubo T. Static and dynamic biomechanical properties of the regenerating rabbit Achilles tendon. Clin Biomater 2008;32:832–8.
[59] Reddy GK, Stehno-Bittel L, Enwemeka CS. Matrix remodeling in healing rabbit Achilles tendon. Wound Repair Regen 1999;7:518–27.